

A Novel Approach for Improving the PQ in SPIM

P. Jenitha Deepa* and H. Habeebullah Sait

Department of Electrical and Electronics Engineering, University College of Engineering, Anna University (BIT CAMPUS), Trichy, 620 024, India

*Corresponding Author: P. Jenitha Deepa. Email: jenithaelsen@gmail.com

Received: 28 March 2022; Accepted: 28 April 2022

Abstract: Single Phase Induction Motor (SPIM) is widely used in industries at starting stage to provide high starting torque. The objective of the work is to develop a drive for Single Phase Induction Motor that does not use a start or run capacitor. In this work, the researchers present the details about Maximum Power Point Tracking using series-compensated Buck Boost Converter, resonant Direct Current (DC) to Alternate Current (AC) inverter and matrix converter-based drive. The proposed method provides a variable starting torque feature that can be adjusted depending upon machine load to ensure Power Quality (PQ). The system uses Series Compensated Buck Boost Converter (SCBBC) to derive the power from solar source and a Partial Resonant Inverter (PRI) between the Matrix Converter (MC) and DC link battery to reduce the switching loss. The application of Space Vector Pulse Width Modulation (SVPWM) ensures the improvement of power quality at driving terminals of SPIM. The proposed system has been mathematically modelled and simulated in MATLAB SIMULINK environment and was validated using standardized experimental verification.

Keywords: Solar PV source; Series Compensated Buck Boost Converter (SCBBC); Partial Resonant Inverter (PRI); Matrix Converter(MC); Single Phase Induction Motor (SPIM)

1 Introduction

In recent times, the requirement for capacitor is alleviated whereas the matrix converter itself produces the required two currents that are orthogonal to each other [1]. The proposed method provides a variable starting torque feature that can be adjusted depending upon the load on machine.

Besides, the power is derived from Solar Photo Voltaic (SPV) source that uses SPV panels to generate the required power rating [2]. The proposed system uses a series-compensated Buck Boost Converter at the front end at which the Maximum Power Point Tracking (MPPT) is implemented. In the experimental setup, a battery backup is also provided. Resonant converter, connected across the battery, converts the Direct Current (DC) voltage derived from battery into a high voltage high frequency Alternating Current (AC) across the AC link.



This work is licensed under a Creative Commons Attribution 4.0 International License, which permits unrestricted use, distribution, and reproduction in any medium, provided the original work is properly cited.

A 2-by-3 matrix converter accepts the high frequency AC link voltage and produces a set of two AC output voltages that are orthogonal to each other, with respect to a common terminal. The orthogonality, produced by the Matrix Converter, eliminates the need for a starting capacitor.

In current study, the researchers present the details with regards to Maximum Power Point Tracking using series-compensated Buck Boost Converter, resonant DC to AC inverter and matrix converter-based drive. The block schema of the proposed system is shown in Fig. 1.

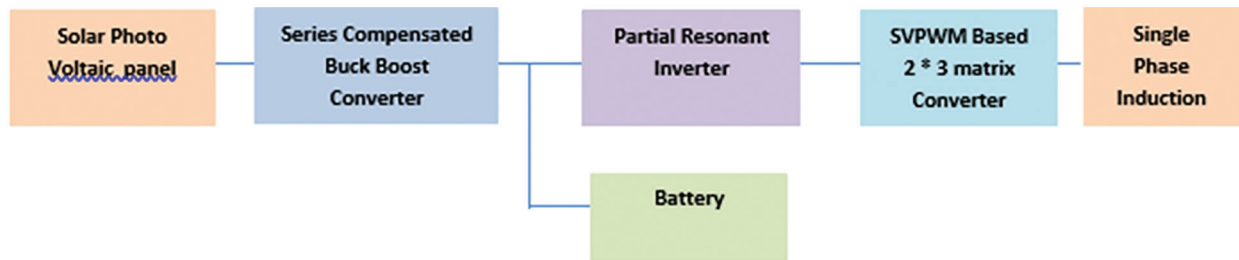


Figure 1: Block schema of solar photo voltaic power harvesting system

An appropriate battery backup with competent ampere hour capacity is used in between the original source of energy and the load. Further, a series-compensated Buck Boost Converter is used between the source and the battery. This converter is meant for the implementation of MPPT. There exists two converters between the load and the battery. The battery drives the partial resonant inverter whereas this inverter drives the 2-by-3 matrix converter. The output of the partial resonant inverter is AC and its frequency lies in the order of 5 kHz. The matrix converter accepts this high frequency AC and delivers a 3-phase AC output with variable frequencies and amplitude features. By controlling the modulation index of matrix converter, the power output of the single phase motor can be adjusted.

The speed of the single phase motor is regulated by a Proportional–Integral (PI) controller at 1450 Revolutions Per Minute (RPM). The proposed system has been mathematically modelled and simulated in MATLAB SIMULINK environment and the same was validated using appropriate experimental verification.

In current work, the researcher discussed about MPPT using the series-compensated BBC, resonant DC to AC inverter and MC-based drive. The proposed method provides a variable starting torque feature that can be adjusted based on machine load in order to ensure Power Quality (PQ). The system uses Series-Compensated Buck Boost Converter (SCBBC) to derive power from solar source, and a Partial Resonant Inverter (PRI) between the Matrix Converter (MC) and DC link battery to reduce the switching loss. The application of Space Vector Pulse Width Modulation (SVPWM) ensures the improvement of power quality at driving terminals of Single Phase Induction Motor.

2 Solar Photo Voltaic Energy Harvesting Sub System

The proposed system uses solar photovoltaic energy as a sole energy source for operating a pump driven by Single Phase Induction Motor. During day time, the harvested solar PV energy is routed to the load and also to lead acid battery-based energy storage system [3].

The Series Compensated Buck Boost Converter (SCBBC) is placed in between the SPV unit and the battery. This converter is required so as to implement the MPPT and it acts as an interface between SPV and the battery. Battery is a voltage sink and its terminal voltage is fairly constant compared to possible voltage variations observed across the SPV subsystems [4]. SCBBC is driven in such a manner that the

terminal voltage of SPV subsystem is maintained at an optimal value. This optimal value is required for harvesting the maximum possible power [5] from SPV for the given solar insolation. The advantage of SCBBC is that the complete power harvested by the SPV system need not flow through SCBBC, but only a part of the power harvested needs to be routed through SCBBC. Rest of the part can be allowed to flow directly to the load [6]. This helps in reduction of size or electrical capacity required by SCBBC for harvesting and transacting the given power.

2.1 Maximum Power Point Tracking

SPV subsystem is expected to generate a maximum of 2 KW. The maximum generated power i.e., 2 kW is used to drive the single phase pump and charge the lead acid battery-based energy storage system. SPV subsystem consists of 15 solar panels. Out of 15 SPV panels, three parallel strings are formed. In each string, five panels are connected in series. The specifications of one of the panels used in SPV subsystem is shown in [Tab. 1](#).

Table 1: Specifications of a single panel

Parameters	Specification of a single panel
Rated maximum power	125.1432 W
Open circuit voltage	21.58 V
Short circuit current	7.89 A
Voltage at pmax	17.19 V
Current at pmax	7.28 A

With three strings in parallel and five panels in series for every string, the overall specifications are shown in [Tab. 2](#).

Table 2: Overall specifications of the panels

Parameters	Specification
Rated maximum power	$125.1432 * 15 = 1877.142 \text{ W}$
Open circuit voltage	$21.58 \text{ V} * 5 = 107.9 \text{ V}$
Short circuit current	$7.89 \text{ A} * 3 = 23.67 \text{ A}$
Voltage at pmax	$17.19 \text{ V} * 5 = 85.95 \text{ V}$
Current at pmax	$7.28 \text{ A} * 3 = 21.84 \text{ A}$

The voltage power characteristics' and voltage current characteristics' families for one of the PV panels are shown in [Figs. 2](#) and [3](#).

3 Series-Compensated Buck Boost Converter (SCBBC)

Series Compensated Buck Boost converter is a DC-to-DC converter with voltage gain characteristics similar to DC-to-DC Generic Boost Converter (GBC). Topologically, SCBBC is similar to that of Generic Buck Boost Converter (GBBC). GBBC has a special advantage i.e., the polarity of DC output voltage is in opposite direction compared to the polarity of its source voltage. This feature makes it possible to treat

both source voltage and the voltage across the output capacitor to act in series. So, it is possible to show that the voltage gain of SCBBC is the same alike GBC. The output of SCBBC is drawn across the positive terminal of the source and negative terminal of the load. SCBBC combines the features of both GBBC and GBC. This section discusses the topology of SCBBC, derivation of its voltage gain from the first principle, and its state space analysis.

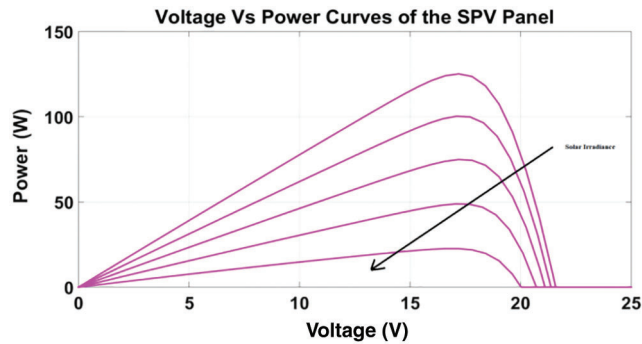


Figure 2: Family of curves relating terminal voltage and the power output of SPV panel

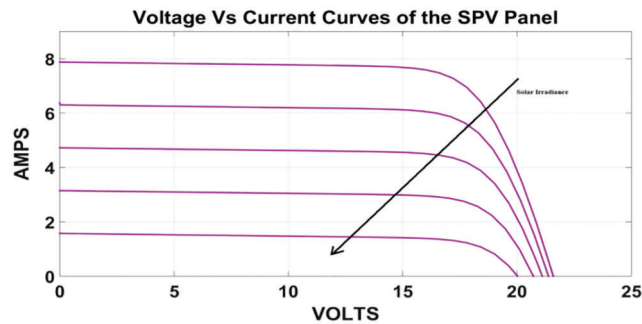


Figure 3: Family of curves relating terminal voltage and the solar PV panel current

The three basic DC-to-DC converters are buck converter, boost converter and Buck Boost Converter (BBC) [7]. In case of buck and boost converters, both input and the output share a common negative terminal. In case of Buck Boost Converter, the input and the output share a common terminal. This common terminal remains the negative terminal for the input whereas it remains the positive terminal for the output. SCBBC delivers the output power across the positive terminal of the source and the negative terminal of normally-connected capacitor on output side. The voltage gain for SCBBC can be derived as given herewith.

With reference to the circuit diagram shown in Fig. 4, the topology is much similar to Buck Boost Converter. The voltage gains of Buck Boost topology, considering the input voltage V_{in} and voltage across the output capacitor V_{out} , is given by the standard equation given herewith.

$$\text{Voltage Gain}(K) = \frac{D}{1-D},$$

where K is the voltage gain and D is the duty cycle. Therefore, the output voltage is calculated as follow; $V_{out} = K * V_{in}$. In case of SCBBC, the output voltage is the sum of input voltage (V_{in}) and output

voltage (V_{out}). Therefore, the output voltage of SCBBC can be denoted by V_L and the voltage across the load can be expressed in the Eqs. (1) and (2)

$$V_L = (V_{in} + V_{out}) = (V_{in}) + \left(V_{in} * \left(\frac{D}{1-D} \right) \right). \tag{1}$$

$$= \frac{(V_{in} * (1 - D)) + (V_{in} * D)}{1 - D} = \frac{V_{in} - V_{in} * D + V_{in} * D}{1 - D} = \frac{V_{in}}{1 - D} \tag{2}$$

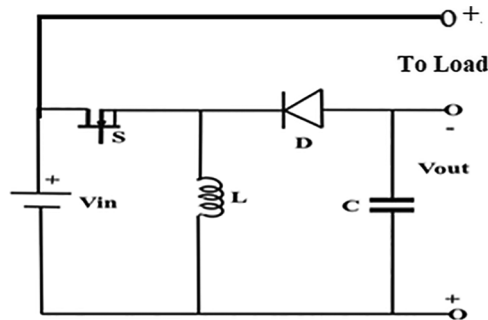


Figure 4: Topology of series-compensated buck boost converter

Thus, the voltage gain equation of the SCBBC is derived as the same alike Generic Boost Converter. However, SCBBC is more advantageous than GBC in such a way that the total power, transacted to the load from the source, is not completely transacted through the converter. While, only a part of the total power flows through the converter, the remaining part flows directly to the load. This leads to reduction in losses as well capacities or sizes of the components required.

Going by an example, the following calculations are applied. Let $V_{in} = 60\text{ V}$ and $D = 0.5$. With generic Buck Boost Converter, the output voltage that appears across the capacitor will be $V_{out} = V_{in} * \frac{D}{1-D} = 60 * \frac{0.5}{1-0.5} = 60\text{ V}$. The overall output voltage, available for the load, is the sum of voltage across the output capacitor. Therefore, the input voltage is $60\text{ V} + 60\text{ V} = 120\text{ V}$. By applying the voltage gain equation of generic boost converter, i.e., $V_{out} = V_{in} * \left(\frac{D}{1-D} \right)$, the output voltage comes out to be 120 V . The studies related to the transient response, of any power electronic converter, are easily conducted with the help of state space analysis [8–11]. Both inductor L and capacitor C are two storage elements whereas the current through the inductor I_L and the voltage across the capacitor V_C are two state variables [6,7].

3.1 The Resonant Frequency Calculation

A switching frequency of nearly 8 KHz has been selected for current study. Both L and C values are chosen so that the frequency of oscillation reaches 11.2 KHz approximately. In this work, the selected values of L and C 0.1 mH and $2E-6$ respectively.

According to the fundamental formula for frequency of oscillation in a parallel resonant circuit,

$$f_o = \frac{1}{2\pi\sqrt{LC}} = 11.2\text{ kHz}$$

Here, the current to load circuit is a constant. When load side current is sinusoidal, no current is drawn from the PRI [12–15]. The matrix converter, used for driving the Single Phase Induction Motor, is realized. The matrix converter is fed with alternating AC link voltage that appears at the output of PRI [16]. The complete power, required by Single Phase Induction Motor, is supplied by the AC link with parallel LC resonant circuit. In the beginning, as the machine draws heavy current, the AC link voltage falls to the least value and reaches as low as 180 V [17–20]. Further, due to increasing torque at the beginning, the speed also increases. However, in later stage, the torque falls and the motor maintains its speed at a required 1450 RPM level as shown in Fig. 5. The phase shift that occurs at 90 degrees between the Main winding and Auxiliary winding is clearly shown in Fig. 6.

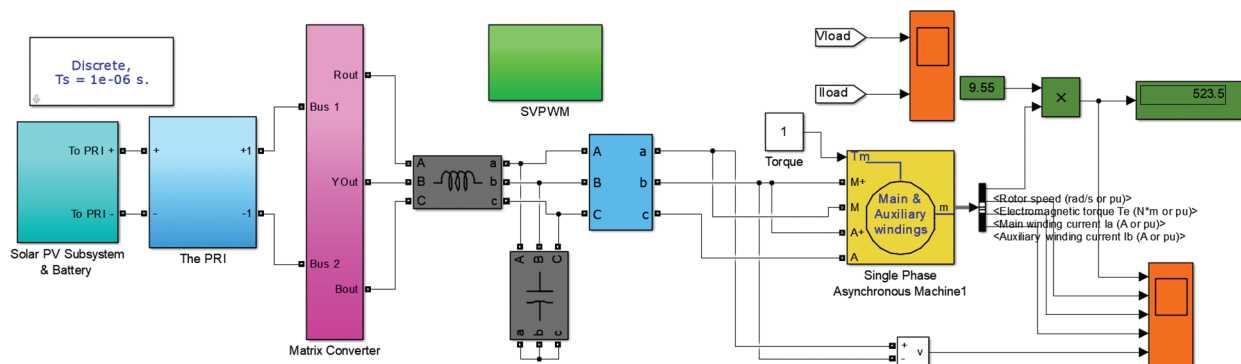


Figure 5: Overall subsystem of the proposed system

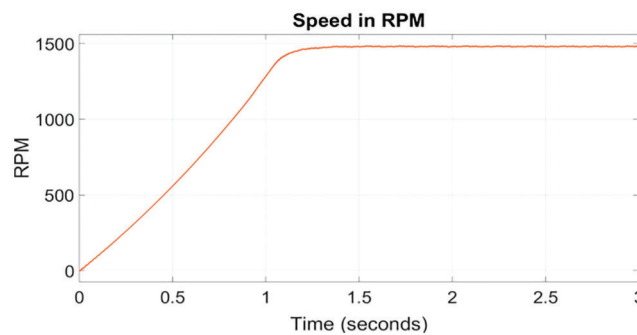


Figure 6: The speed of single phase induction motor regulated at 1450 RPM

Gradually, upon the completion of start-up that takes as much as 1.5 s, the motor speed becomes a constant. Then, the torque also comes down and the AC link voltage reaches its maximum value of 400 V. These effects are clearly perceivable from the Figs. 7–9.

4 Experimental Verification

In the current study experimental setup, SPV panel and the battery are low voltage ones which are rated typically with nominal voltage ratings of 18 V and 12 V. The output voltage, across the resonant inverter, is 60 V. This 60 V AC bus was applied as the input to matrix converter. A photo graph of the experimental setup, to validate the proposed idea, is shown in Fig. 10. The detailed specifications of the components are shown in Tab. 3. Figs. 11–12 show the switching pulses to cross arms of PRI with MI values such as 0.2 and 0.45 respectively.

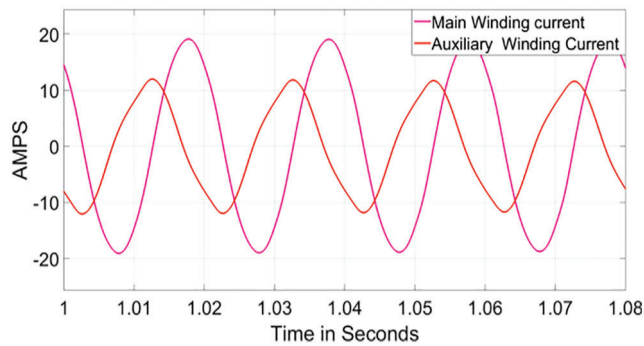


Figure 7: The main and auxiliary winding currents showing 90 degrees’ displacement

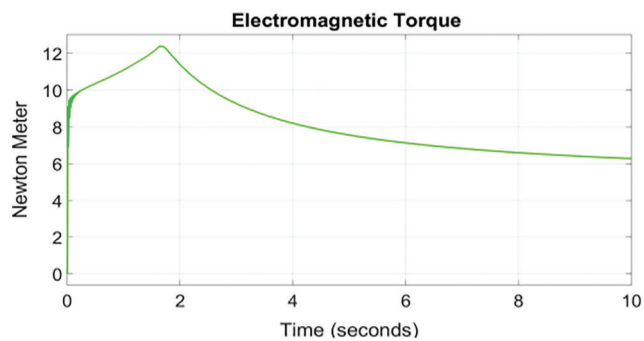


Figure 8: The main and auxiliary winding currents showing 90 degrees’ displacement

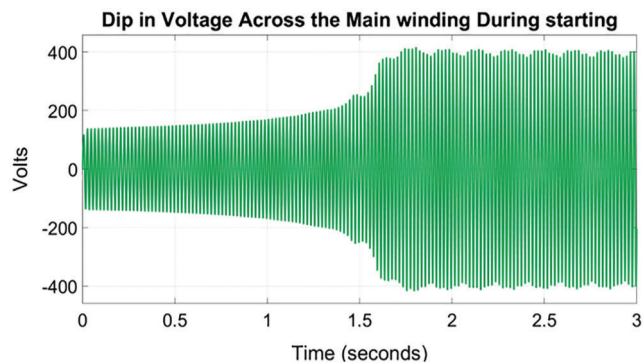


Figure 9: The fall and rise of AC link voltage during the starting transient of Single Phase Induction Motor

Fig. 13 shows the output voltage that appears across the AC link. With low modulation index, the amplitude of the AC link got reduced. With modulation index as high as 0.45, the amplitude of the AC link voltage was very high as shown in Fig. 14. In Fig. 15, the spectrum of the resonant AC link voltage is shown. Due to partial resonant nature, the spectrum exhibited harmonics with fundamentals placed at switching frequency.

Figs. 16 and 17 show 3-phase and single phase AC output voltages across three phase nodes of the matrix converter. This three phase output remains the driving voltage for Single Phase Induction Motor.

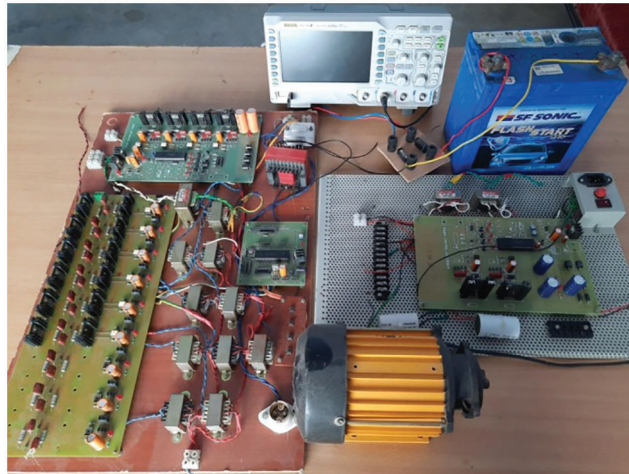


Figure 10: Proposed system experimental prototype

Table 3: Component specification

Component	Specifications
Solar PV module	
Rated power	125 W 2 Nos. parallel
SCBBC	
MOSFET	IRF 840
Inductor L	1 Mh
Battery	35 AH Lead Acid
Nominal voltage	12 V
Partial resonant inverter	12 kHz
MOSFET	IRF 840 4 Nos.
Diodes	6 A
Inductor L	1 mH
Capacitor C	2 MFD
Zero crossing detector	LM 741
Matrix converter	
MOSFETs	IRF 840 B to B 6 Modules
Single phase induction motor	185 W 230 V 50 Hz
Rated speed	1450 RPM

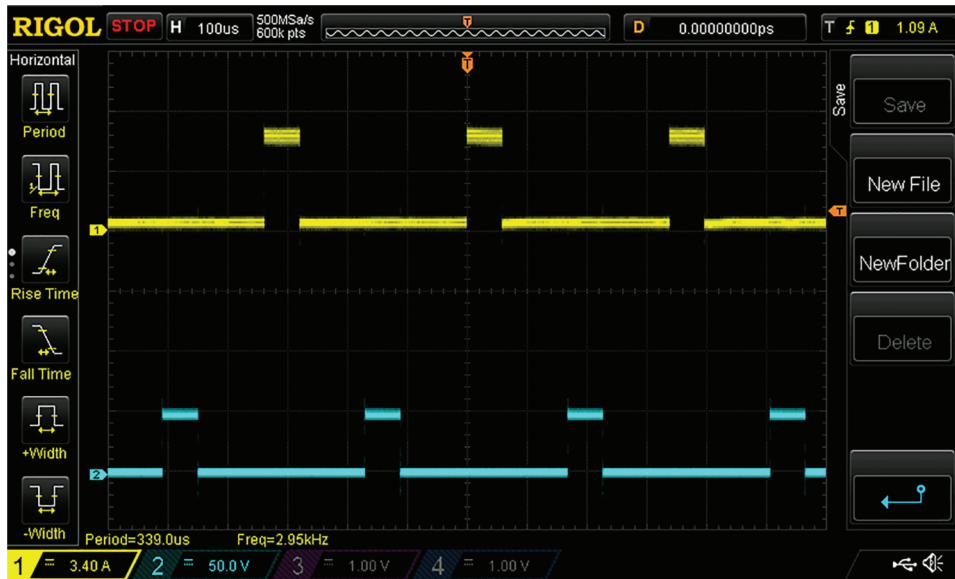


Figure 11: Switching pulses to the cross arms of PRI with an MI of 0.2

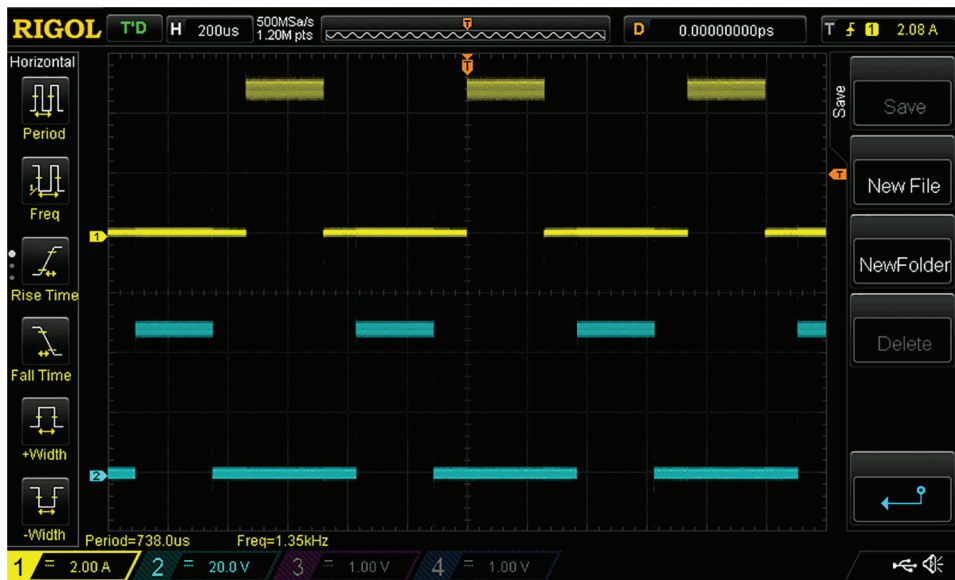


Figure 12: Switching pulses to the cross arms of PRI with an MI of 0.45



Figure 13: AC link voltage across LC network at PRI output



Figure 14: Spectrum of AC link voltage with MI = 0.45



Figure 15: Spectrum of AC link voltage with MI = 0.2

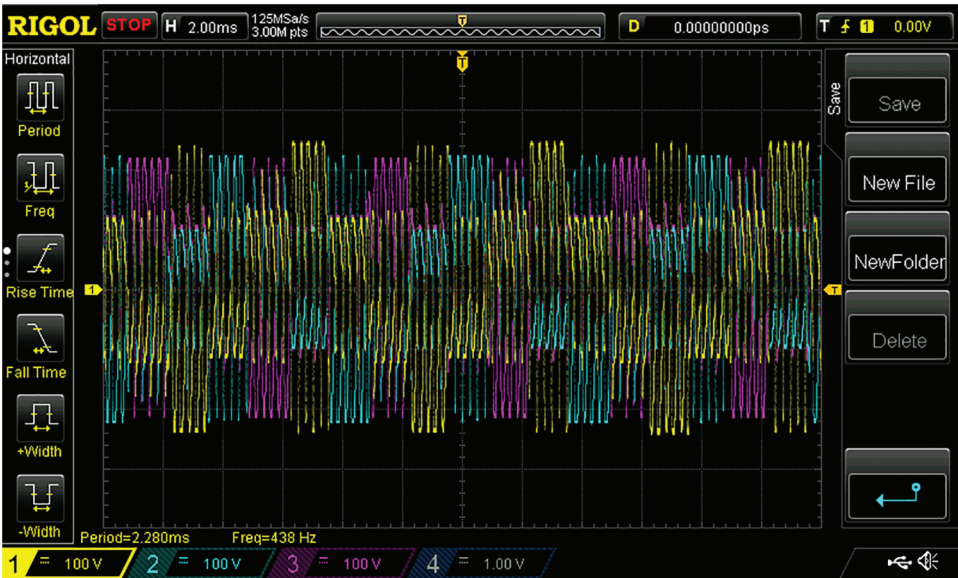


Figure 16: Three-phase AC output voltage of matrix converter



Figure 17: Spectrum of one of the R-phase voltage outputs of matrix converter

5 Conclusion

In this work, a solar photo voltaic-powered drive has been presented for Single Phase Induction Motor. The proposed system includes a SCBBC at front end to harvest the solar photo voltaic energy with Maximum Power Point Tracking. In comparison with generic boost converter that offers the same voltage gain, SCBBC is highly efficient and less prone for inductor saturation. For SCBBC, the ratings of the components required are less than the Generic Boost converter. Further, a partial Resonant Inverter is used in between the matrix converter and DC link battery. Using a high frequency partial resonant inverter ensures zero voltage switching on the inverter side which reduces the switching losses. The size of LC unit is smaller and is light weight than the conventional two winding transformer. The application of SVPWM improves the power quality at driving terminals of Single Phase Induction Motor. Considering these advantages, the researchers suggest that SCBBC can be used in SPV power harvesting stage in future with a PRI in inverter stage and a MATRIX converter in final inverter stage.

Funding Statement: The authors received no specific funding for this study.

Conflicts of Interest: The authors declare that they have no conflicts of interest to report regarding the present study.

References

- [1] B. Bendib, H. Belmili and F. Krim, "A survey of the most used MPPT methods: Conventional and advanced algorithms applied for photovoltaic systems," *Renewable and Sustainable Energy Reviews*, vol. 45, no. 8, pp. 637–648, 2015.
- [2] H. Rezk and A. M. Eltamaly, "A comprehensive comparison of different MPPT techniques for photovoltaic systems," *Solar Energy*, vol. 112, no. 2, pp. 1–11, 2015.
- [3] L. M. Elobaid, A. K. Abdelsalam and E. E. Zakzouk, "Artificial neural network-based photovoltaic maximum power point tracking techniques: A survey," *IET Renewable Power Generation*, vol. 9, no. 8, pp. 1043–1063, 2015.
- [4] L. L. Jiang, D. R. Nayanisiri, D. L. Maskell and D. M. Vilathgamuwa, "A hybrid maximum power point tracking for partially shaded photovoltaic systems in the tropics," *Renewable Energy*, vol. 76, pp. 53–65, 2015.

- [5] H. J. El-Khozondar, R. J. El-Khozondar, K. Matter and T. Suntio, "A review study of photovoltaic array maximum power tracking algorithms," *Renewables*, vol. 3, no. 1, pp. 3, 2016.
- [6] H. M. El-Helw, A. Magdy and M. I. Marei, "A hybrid maximum power point tracking technique for partially shaded photovoltaic arrays," *IEEE Access*, vol. 5, pp. 11900–11908, 2017.
- [7] F. Belhachat and C. Larbes, "Global maximum power point tracking based on ANFIS approach for PV array configurations under partial shading conditions," *Renewable and Sustainable Energy Reviews*, vol. 77, no. 4, pp. 875–889, 2017.
- [8] D. S. Padimiti, M. B. Christian and J. Jarvinen, "Effective transient-free capacitor switching (TFCS) for large motor starting on MV systems," in *2017 Petroleum and Chemical Industry Technical Conf. (PCIC)*, Calgary, AB, pp. 113–124, 2017.
- [9] P. P. Rajeevan, K. Sivakumar, C. Patel, R. Ramchand and K. Gopakumar, "A seven-level inverter topology for induction motor drive using two-level inverters and floating capacitor fed h-bridges," *IEEE Transactions on Power Electronics*, vol. 26, no. 6, pp. 1733–1740, 2011.
- [10] S. Rahman, M. Meraj, A. Iqbal, M. Tariq, A. I. Maswood *et al.*, "Cascaded multilevel qZSI powered single-phase induction motor for water pump application," in *2017 IEEE Energy Conversion Congress and Exposition (ECCE)*, Cincinnati, OH, pp. 1037–1042, 2017.
- [11] S. Jain, A. K. Thopukara, R. Karampuri and V. T. Somasekhar, "A single-stage photovoltaic system for a dual-inverter-fed open-end winding induction motor drive for pumping applications," *IEEE Transactions on Power Electronics*, vol. 30, no. 9, pp. 4809–4818, 2015.
- [12] N. K. Kumar and K. Sivakumar, "A quad two-level inverter configuration for four-pole induction-motor drive with single dc link," *IEEE Transactions on Industrial Electronics*, vol. 62, no. 1, pp. 105–112, 2015.
- [13] M. Guo, Y. Liu, B. Ge, S. Liu, X. Li *et al.*, "Quasi-Z source indirect matrix converter-fed induction motor drive," *IET Electric Power Applications*, vol. 14, no. 5, pp. 797–808, 2020.
- [14] J. Jongudomkarn, J. Liu, Y. Yanagisawa, H. Bevrani and T. Ise, "Model predictive control for indirect boost matrix converter based on virtual synchronous generator," *IEEE Access*, vol. 8, pp. 60364–60381, 2020.
- [15] T. N. Mir, B. Singh and A. H. Bhat, "Improvised multi-objective model predictive control of matrix converter using fuzzy logic and space vectors for switching decisions," *IET Power Electronics*, vol. 13, no. 4, pp. 758–764, 2020.
- [16] E. L. Robles, J. J. R. Rivas, E. P. Sánchez and O. C. Castillo, "Voltage regulation of a matrix converter with balanced and unbalanced three-phase loads," *Journal of Applied Research and Technology*, vol. 13, no. 5, pp. 510–522, 2015.
- [17] A. Djahbar, B. Benziane and A. Zegaoui, "A novel modulation method for multilevel matrix converter," *Energy Procedia*, vol. 50, pp. 988–998, 2014.
- [18] S. M. Dabour, A. S. A. Khalik, S. Ahmed, A. M. Massoud and S. M. Allam, "Common-mode voltage reduction for space vector modulated three- to five-phase indirect matrix converter," *International Journal of Electrical Power & Energy Systems*, vol. 95, no. 1, pp. 266–274, 2018.
- [19] N. G. M. Thao, K. Uchida and N. Nguyen-Quang, "An improved incremental conductance-maximum power point tracking algorithm based on fuzzy logic for photovoltaic systems," *SICE Journal of Control, Measurement, and System Integration*, vol. 7, no. 2, pp. 122–131, 2014.
- [20] S. Shabaan, M. I. A. E. Sebah and P. Bekhit, "Maximum power point tracking for photovoltaic solar pump based on ANFIS tuning system," *Journal of Electrical Systems and Information Technology*, vol. 5, no. 1, pp. 11–22, 2018.